Modeling, Identification and Control, Vol. 45, No. 2, 2024, pp. 41–50, ISSN 1890–1328

Stochastic Sequential Model Predictive Control for Operating Buffer Reservoir in Hjartdøla Hydropower System under Uncertainty

Changhun Jeong [1] Beathe Furenes [2] Roshan Sharma [1]

[1] *Department of Electrical engineering, Information Technology and Cybernetics, University of South-Eastern Norway, Porsgrunn, Norway. E-mail:* changhun.jeong@usn.no / roshan.sharma@usn.no

[2] *Skagerak Kraft AS, Porsgrunn, Norway.*

Abstract

This study focuses on demonstrating the effectiveness and efficiency of the Stochastic Sequential Model Predictive Control (MPC) framework within the context of the Hjartdøla hydropower system. Multistage MPC, while effective in managing uncertainty, poses challenges due to its high computational demands and complex optimal control problems, particularly in applications requiring long-term forecasting, such as hydropower systems. Through a comparative simulation study with multistage MPC, this paper highlights the superior feasibility and computational speed of the Stochastic Sequential MPC framework. This work contributes to the broader understanding of MPC applications in hydropower systems

Keywords: Model predictive control, Stochastic MPC, Uncertainty, Flood management

1 Introduction

Hydropower, esteemed for its environmental benefits(IEA, 2021), confronts challenges that can adversely impact aquatic ecosystems within watercourses(Schmutz and Sendzimir, 2018). Among these challenges, hydropeaking, characterized by abrupt fluctuations in discharged water flow rates from hydropower turbines, poses a significant threat. Hydropeaking incidents often result from operating hydropower stations in response to fluctuating power demand and can have devastating consequences on downstream fauna (Batalla et al., 2021).

To mitigate the ecological harm caused by hydropeaking, the deployment of buffer reservoirs has emerged as a viable solution. The primary objective of buffer reservoirs is to regulate downstream flow rates in a stable manner by temporarily storing or releasing water (Langhans et al., 2019). However, managing these buffer reservoirs is a formidable task due to the presence of stringent operational regulations and inherent uncertainties. These uncertainties encompass factors such as variations in power production plans and fluctuations in water inflow originating from diverse streams and rivers.

The Hjartdøla hydropower system, situated in the Hjartdal municipality of Norway and operated by Skagerak Kraft, encounters similar challenges. This hydropower facility, equipped with two Pelton turbines and a buffer reservoir known as Hjartsjå, is specifically designed to control downstream water flow rates. The operational parameters of the Hjartdøla hydropower plant entail constraints related to the water level at Hjartsjå, flow rates through a floodgate, and downstream conditions. Furthermore, the system contends with multiple sources of uncertainty, including variations in power production plans, uncertainties in water inflow forecasts, and model-related uncertainties (SkagerakKraft, 2022).

doi:10.4173/mic.2024.2.1

Currently, the Hjartdøla system employs a Proportional-Integral (PI) controller for system control, supplemented by manual adjustments of setpoints conducted by on-site personnel. However, this control approach is suboptimal, as it heavily relies on human judgment and predictive assessments of uncertainty, thereby elevating the risk of violating operational constraints. Consequently, Skagerak Kraft AS is actively exploring the application of Model Predictive Control (MPC) frameworks to enhance the precision and efficiency of system control.

Model Predictive Control (MPC) has garnered substantial popularity across both industrial and research domains, particularly for optimizing the operation of constrained multiple-input multiple-output processes. Its efficacy in managing multivariable systems subject to constraints has led to successful implementations in various industrial applications (Morari and Lee, 1999). MPC involves computing an optimal control sequence for the future by solving a finite horizon open-loop Optimal Control Problem (OCP) based on available system information. Subsequently, the first control input in the sequence is applied, and this procedure repeats at regular sampling intervals (Mayne et al., 2000). Notably, MPC has demonstrated utility in addressing the operational constraints of hydropower systems (Jeong et al., 2021; Jeong and Sharma, 2022b), although challenges arise due to the inherent uncertainty associated with water inflow to the reservoir, potentially leading to constraint violations(Jeong et al., 2021).

To mitigate these constraint violations, addressing uncertainty becomes imperative when designing and implementing MPC. One prominent approach is Stochastic MPC, exemplified by the multistage MPC or scenario-based MPC framework (Mesbah, 2016). The genesis of this framework can be traced back to the min-max feedback MPC concept introduced in (Scokaert and Mayne, 1998) and later formalized as multistage MPC by (Lucia et al., 2013). This framework portrays future uncertainty evolution through a discrete-time scenario tree and employs feedback mechanisms, facilitating closed-loop optimization. It tackles the OCP across multiple control trajectories to account for all plausible realizations of uncertainty. Multistage MPC's versatility has been showcased across diverse domains, including chemical process systems(Lucia et al., 2013; Martí et al., 2015), autonomous vehicles(Klintberg et al., 2016), building climate control(Maiworm et al., 2015), and notably, the management of hydropower systems operating under uncertain water inflow conditions (Jeong and Sharma, 2022a; Jeong et al., 2023b; Jeong and Sharma, 2023). However, challenges persist in terms of computational demands and the intricacy of the OCP structure.

To address these challenges inherent in multistage MPC, the Stochastic Sequential MPC framework was introduced in a prior study. This framework orchestrates two sequential optimizations: an initial optimizer akin to the certainty-equivalent MPC framework, followed by a subsequent optimizer that aligns closely with multistage MPC principles. Previous research demonstrated the advantages of enhanced feasibility and expedited computational efficiency in solving OCP, highlighting the benefits of employing the Stochastic Sequential MPC framework over traditional multistage MPC approaches(Jeong et al., 2023a).

This paper endeavors to apply the Sequential Stochastic Model Predictive Control (MPC) framework to the Hjartdøla hydropower system and subsequently assess its efficacy and efficiency in this context.

The paper's organizational structure is as follows: Section 2 offers an introduction to the Sequential Stochastic MPC framework. In Section 3, the study delves into the particulars of the case study and outlines the simulation configurations. Subsequently, Section 4 is dedicated to the presentation of simulation results, accompanied by a comprehensive discussion of the findings. Finally, Section 5 encapsulates the study's conclusions.

2 STOCHASTIC SEQUENTIAL MPC

The stochastic sequential MPC framework bears resemblance to human decision-making processes within the context of long-term project management. In such scenarios, an initial long-term plan is formulated based on available resources, skills, and information, without explicit consideration of future uncertainties. This long-term plan serves as a foundational blueprint for developing short-term action plans on a daily or weekly basis. While the short-term plans align with the long-term strategy, they also incorporate provisions for potential issues or uncertainties that might arise. In essence, the short-term plans strive to adhere as closely as possible to the long-term plan, while concurrently integrating contingency plans for unforeseen events. This iterative planning approach facilitates the effective and efficient management of long-term projects (Jeong et al., 2023a).

The framework of stochastic sequential MPC, as depicted in Figure 1, amalgamates characteristics from both the certainty-equivalent MPC framework and the multistage MPC framework. In this framework, the first optimizer functions akin to the certainty-equivalent MPC framework, generating a long-term reference control sequence denoted as $\mathbf{U}^*_{\mathrm{ref}}$. This ref-

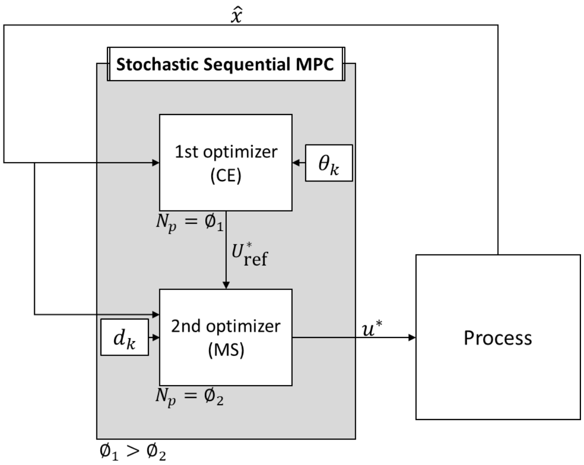

Figure 1: The framework of Stochastic Sequential MPC (Jeong et al., 2023a)

erence control sequence is computed over a prediction horizon of length $N\text{p} = \phi_1$, predicated on nominal values of uncertainty denoted as θ_k, and the measured or estimated system states denoted as $\hat{\mathbf{x}}$. Conversely, the second optimizer resembles the multistage MPC framework, producing short-term optimal control sequences by considering presently available scenarios of uncertainty in the future, denoted as $\mathbf{d}_k$, while also aiming to track the long-term reference control sequence, $\mathbf{U}^*_{\text{ref}}$, generated by the first optimizer. The optimal control sequence within the second optimizer is computed over a shorter prediction horizon of length $N_\text{p} = \phi_2$, where ϕ_2 is significantly shorter than ϕ_1 (Jeong et al., 2023a).

Despite not explicitly addressing uncertainty in the distant future, the stochastic sequential MPC framework incorporates future uncertainty information by the second optimizer. Consequently, stochastic sequential MPC can achieve control performance akin to multistage MPC, while demanding less computational resources and enhancing the feasibility of the optimal control problem (Jeong et al., 2023a).

Let's consider a discrete-time nonlinear system, described by the following equation

$$\mathbf{x}_{k+1} = \mathbf{f}(\mathbf{x}_k, \mathbf{u}_k, \mathbf{d}_k) \tag{1}$$

In this equation, $\mathbf{x}_k \in \mathbb{R}^{n_x}$ represents the system states at time step k, $\mathbf{u}_k \in \mathbb{R}^{n_u}$ represents the control inputs at the same time step, and $\mathbf{d}_k$ denotes the ensemble of scenarios representing uncertainty over the prediction horizon, available at time step k. This relationship can be expressed as:

$$\mathbf{d}_k = \begin{pmatrix} \mathbf{d}_k^{(1)} & \cdots & \mathbf{d}_k^{(S)} \\ \vdots & \ddots & \vdots \\ \mathbf{d}_{k+N_\text{p}}^{(1)} & \cdots & \mathbf{d}_{k+N_\text{p}}^{(S)} \end{pmatrix} \tag{2}$$

Here, S represents the number of scenario ensembles, with each column representing a distinct scenario ensemble. The formulation of the first optimizer mirrors that of the certainty-equivalent MPC, taking the following form:

$$\begin{aligned} \text{minimize} \quad & \sum_{k=0}^{\phi_1} \mathbf{J}(\mathbf{x}_k, \mathbf{u}_k, \theta_k) && \text{(3a)} \\ \text{subject to} \quad & \mathbf{x}_0 = \hat{\mathbf{x}}, && \text{(3b)} \\ & \mathbf{x}_{k+1} = \mathbf{f}(\mathbf{x}_k, \mathbf{u}_k, \theta_k), && \text{(3c)} \\ & \mathbf{g}(\mathbf{x}_k, \mathbf{u}_k, \theta_k) \leq 0, && \text{(3d)} \\ & \mathbf{x}_\text{lb} \leq \mathbf{x}_k \leq \mathbf{x}_\text{ub}, && \text{(3e)} \\ & \mathbf{u}_\text{lb} \leq \mathbf{u}_k \leq \mathbf{u}_\text{ub} && \text{(3f)} \end{aligned}$$

Where θ_k represents the nominal value of the uncertainty d_k, and $\hat{\mathbf{x}}$ denotes the measured or estimated states. The initial state for the optimization problem is provided in equation (3b). The system model and output constraints are integrated into equations (3c) and (3d), respectively. The bounds on states and control inputs are enforced through equations (3e) and (3f). The prediction horizon length, denoted as N_p, is set to ϕ_1 with $k = 0, 1, \ldots, \phi_1$ (Jeong et al., 2023a).

As a result of the first optimization, the reference control sequence is derived as $\mathbf{U}^*_\text{ref} = [\mathbf{U}^*_{\text{ref},1}, \ldots, \mathbf{U}^*_{\text{ref},\phi_2}, \ldots, \mathbf{U}^*_{\text{ref},\phi_1}]$. A portion of this reference control sequence, specifically $[\mathbf{U}^*_{\text{ref},1}, \ldots, \mathbf{U}^*_{\text{ref},\phi_2}]$, is passed to the second optimizer. The formulation of the second optimizer closely resembles that of the multistage MPC framework, taking the following form:

$$\begin{aligned} \text{minimize} \quad & \sum_{j=1}^{S} \omega_j \sum_{k=0}^{\phi_2} \mathbf{J}(\mathbf{x}_k^j, \mathbf{u}_k^j, \mathbf{d}_k^j) + Q_u(\mathbf{u}_k^j - \mathbf{U}^*_{\text{ref},k})^2 && \text{(4a)} \\ \text{subject to} \quad & \mathbf{x}_0^j = \hat{\mathbf{x}}, && \text{(4b)} \\ & \mathbf{x}_{k+1}^j = \mathbf{f}(\mathbf{x}_k^j, \mathbf{u}_k^j, \mathbf{d}_k^j), && \text{(4c)} \\ & \mathbf{g}(\mathbf{x}_k^j, \mathbf{u}_k^j, \mathbf{d}_k^j) \leq 0, && \text{(4d)} \\ & \mathbf{x}_\text{lb} \leq \mathbf{x}_k^j \leq \mathbf{x}_\text{ub}, && \text{(4e)} \\ & \mathbf{u}_\text{lb} \leq \mathbf{u}_k^j \leq \mathbf{u}_\text{ub}, && \text{(4f)} \\ & \mathbf{u}_k^j = \mathbf{u}_k^l \quad \text{if} \quad \mathbf{x}_k^{p(j)} = \mathbf{x}_k^{p(l)} && \text{(4g)} \end{aligned}$$

In this context, Q_u serves as a weight parameter governing the tracking of the reference control sequence,

Table 1: Parameters for Lake Toke model

Parameter	Value	Unit	Comment
LRV	155.7	m MSL	Lower regulated value
HRV	157.5	m MSL	Higher regulated value
$h_{\mathrm{in,max}}$	$HRV + 3 - LRV = 4.8$	m	Maximum water level of the buffer reservoir (Hjartsjå)
A_{min}	10^3	m^2	Minimum surface area of water in the buffer reservoir (Hjartsjå)
a	0.0474	-	Coefficient
b	1.6898	-	Coefficient
$h^{\mathrm{msl}}_{\mathrm{g,top}}$	157.37	m MSL	Top position of gate opening
L_1	12	m	Width of the gate
L_2	11	m	Width of the overflow channel
OFT^{msl}_1	157.5	m MSL	Overflow threshold 1
OFT^{msl}_2	158.5	m MSL	Overflow threshold 2

while ω_j represents the weight or probability associated with the j^{th} scenario ensemble (Jeong et al., 2023a).

The initial states for all scenario ensembles in the optimization problem are provided by equation (4b). The system model and output constraints are integrated into equations (4c) and (4d), respectively. Bounds on states and control inputs are enforced through equations (4e) and (4f) (Jeong et al., 2023a).

The non-anticipativity constraint, as articulated in (4g), ensures that the same control inputs are applied at parent nodes where scenarios branch out. Here, l represents a scenario number distinct from j. The prediction horizon N_{p} is set as ϕ_2, which is shorter than ϕ_1, with $k = 0, 1, \ldots, \phi_2$. Consequently, a new optimal control sequence is computed over the horizon length ϕ_2 and its first control input is applied to the system (Jeong et al., 2023a).

For a system characterized by n_x states and n_u control inputs, the multistage MPC framework necessitates solving an Optimization Control Problem (OCP) with $(n_x + n_u) \cdot N_{\mathrm{p}} \cdot S$ variables. Here, S denotes the number of available scenarios of uncertainty over the prediction horizon length N_{p}. In contrast, the stochastic sequential MPC framework addresses two OCPs sequentially. The first OCP involves $(n_x + n_u) \cdot N_{\mathrm{p}}$ variables, while the second OCP encompasses $(n_x + n_u) \cdot \phi_2 \cdot S$ variables. Consequently, the sizes of the OCPs in stochastic sequential MPC are reduced by factors of $1/S$ and ϕ_2/N_{p} compared to one in multistage MPC, resulting in decreased computational demands (Jeong et al., 2023a).

3 CASE STUDY

3.1 System description

Hjardøla hydropower plant has two Pelton turbines of 60MW each. After the turbines, there is a buffer reservoir, called Hjartsjå, which is used to control the water flow rate at downstream SkagerakKraft (2022). Figure. 2 displays a layout of the Hjartdøla hydropower system and Figure. 3 shows the structure of the Hjartsjå buffer reservoir. The water flows into Hjartsjå from two places: the Hjartdøla hydropower turbines $\dot{V}_{\mathrm{p}}$ and Hjartsjå river $\dot{V}_{\mathrm{i,H}}$. The water flows out from Hjartsjå through a floodgate $\dot{V}_{\mathrm{g}}$ and flood threshold

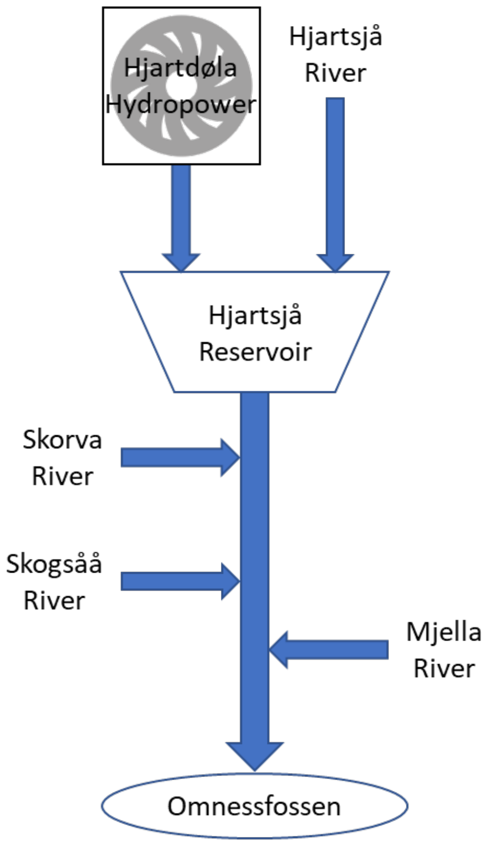

Figure 2: The simple layout of the watercourse system at Hjartdøla hydropower plant

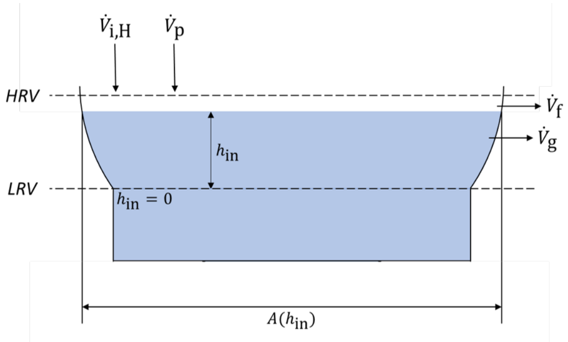

Figure 3: The structure of the Hjartsjå reservoir

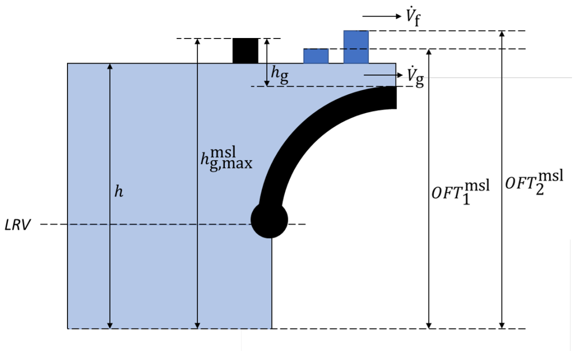

Figure 4: The structure of the floodgate at Hjartsjå reservoir

walls $\dot{V}_{\mathrm{f}}$. Figure. 4 shows the structure of the floodgate at the reservoir. The water flows toward Omnessfossen located in downstream. Between Hjartsjå and Omnessfossen, three main rivers flow into the watercourse: Skorva river $\dot{V}_{\mathrm{i,SV}}$, Skogsåå river $\dot{V}_{\mathrm{i,SS}}$, and Mjella river $\dot{V}_{\mathrm{i,M}}$. The system has two types of uncertainties: the power production plan and the water inflow forecasts from all four rivers. The flow rate forecasts of all rivers are computed based on hydrological models of the rivers and weather forecast information. Each forecast has 50 possible scenario ensembles for the next 13 days (312 hours). The power production plan is the result of the optimization of factors such as electricity price, demand, etc. During the operation, it is important to consider all forecast information to avoid drastic changes in flow rates.

In the model, the state is the water level at the reservoir h, and the control input is the gate opening h_{g}. The parameters of the model are specified in Table. 1 and the model is as follows:

$$h_{\mathrm{in}} = \min(\max(0, h - LRV), h_{\mathrm{in,max}}) \tag{5}$$

$$A(h_{\mathrm{in}}) = \max(A_{\min}, 10^6 \cdot a \cdot b \cdot h_{\mathrm{in}}^{(b-1)}) \tag{6}$$

$$h_{\mathrm{out,g}} = \max(0, h - (h^{\mathrm{msl}}_{\mathrm{g,top}} - h_{\mathrm{g}})) \tag{7}$$

$$\dot{V}_{\mathrm{g}} = 1.84 \cdot L_1 \cdot h^{1.5}_{\mathrm{out,g}} \tag{8}$$

$$h_{\mathrm{out,OF1}} = \max(0, h - OFT^{\mathrm{msl}}_1) \tag{9}$$

$$h_{\mathrm{out,OF2}} = \max(0, h - OFT^{\mathrm{msl}}_2) \tag{10}$$

$$\dot{V}_{\mathrm{f}} = 1.8(L_1 \cdot h^{1.5}_{\mathrm{out,OF1}} + L_2 \cdot h^{1.5}_{\mathrm{out,OF2}}) \tag{11}$$

$$\dot{V}_{\mathrm{O}} = \dot{V}_{\mathrm{g}} + \dot{V}_{\mathrm{f}} + \dot{V}_{\mathrm{i,SV}} + \dot{V}_{\mathrm{i,SS}} + \dot{V}_{\mathrm{i,M}} \tag{12}$$

$$\frac{dh}{dt} = \frac{1}{A(h_{\mathrm{in}})}(\dot{V}_{\mathrm{i,H}} + \dot{V}_{\mathrm{p}} - \dot{V}_{\mathrm{f}} - \dot{V}_{\mathrm{g}}) \tag{13}$$

Operational constraints are designed to achieve (i) operational safety and (ii) prevention of damage to the environment at downstream. The constraints are regulated by the Norwegian Water Resource and Energy Administration (NVE). The violation of the constraints can cause an enormous fine and other sorts of penalties NVE (2022). Therefore, the constraints must be satisfied. The essential constraints are:

1. The flow rate of the water at downstream(Omnessfossen) must be as steady as possible. This requirement is to keep the fauna and people at downstream safe from hydropeaking or the sudden change in the flow rates or levels at downstream.

2. The water flowing out from the Hjartsjå reservoir should be more than 1.0 m^3/s and more than 2.5 m^3/s at Omnessfossen. This ensures that fish can move freely in the watercourse.

3. The water level at the Hjartsjå reservoir must be maintained between HRV and LRV.

3.2 Optimal control problems

The main purpose of the buffer reservoir is to keep the water flow at downstream as constant as possible. Also, it may be beneficial to keep the water level in the reservoir as high as possible because it gives flexibility to the operation. For example, during the dry season, the reservoir can supply enough water for a longer period to satisfy the required minimum flow rate. The first optimizer computes the reference control sequence with the nominal value of the water inflows. The objective function for the first optimizer is formulated as:

$$J_{1,k} = L_k + \Delta R_k + \Delta VO_k \tag{14}$$

$$L_k = (h_k - HRV) \cdot Q_{\mathrm{h}} \cdot (h_k - HRV)^{\intercal} \tag{15}$$

$$\Delta R_k = (u_k - u_{k-1}) \cdot Q_{\Delta \mathrm{u}} \cdot (u_k - u_{k-1})^{\intercal} \tag{16}$$

$$\Delta VO_k = \Delta \dot{V}_{\mathrm{O}}^{k} \cdot Q_{\mathrm{V}} \cdot \Delta \dot{V}_{\mathrm{O}}^{k\intercal} \tag{17}$$

Equation (15) aims to maximize the water level in the buffer reservoir. Equations (16) and (17) inhibit the changes in the floodgate opening and the flow rate at downstream(Omnessfossen). The OCP of the first optimizer is formed as:

$$\begin{aligned}
\text{minimize} \quad & \sum_{k=0}^{\phi_1} J_{1,k} && \text{(18a)}\\
\text{subject to} \quad & h_0 = \hat{h}, && \text{(18b)}\\
& h_{k+1} = f(h_k, h_{\mathrm{g},k}, \mathrm{mean}(\dot{V}_{\mathrm{i,H}}^{j})), && \text{(18c)}\\
& 1.0 m^3/s \leq \dot{V}_{\mathrm{g},k}, && \text{(18d)}\\
& 2.5 m^3/s \leq \dot{V}_{\mathrm{O},k}, && \text{(18e)}\\
& LRV \leq h_k \leq HRV, && \text{(18f)}\\
& 0 \leq h_{\mathrm{g},k} \leq 1.5 m && \text{(18g)}
\end{aligned}$$

In the second optimizer, the uncertainty of water inflow is included in the optimization and the tracking term to the reference control sequence is added. The objective function of the second optimizer is formulated as:

$$J_{2,k} = J_{1,k}^{j} + Q_u(\mathbf{u}_k^j - \mathbf{U}_{\mathrm{ref},k}^{*})^2 \tag{19}$$

OCP for the second optimizer is formulated as:

$$\begin{aligned}
\text{minimize} \quad & \sum_{j=1}^{S} \omega_j \sum_{k=0}^{\phi_2} J_{2,k} && \text{(20a)}\\
\text{subject to} \quad & h_0^j = \hat{h}, && \text{(20b)}\\
& h_{k+1}^j = f(h_k^j, h_{\mathrm{g},k}^j, \dot{V}_{\mathrm{i,H}}^{j}), && \text{(20c)}\\
& 1.0 m^3/s \leq \dot{V}_{\mathrm{g},k}, && \text{(20d)}\\
& 2.5 m^3/s \leq \dot{V}_{\mathrm{O},k}, && \text{(20e)}\\
& LRV \leq h_k^j \leq HRV, && \text{(20f)}\\
& 0 \leq h_{\mathrm{g},k}^j \leq 1.5 m, && \text{(20g)}\\
& h_{\mathrm{g},1}^1 = h_{\mathrm{g},1}^2 = \cdots = h_{\mathrm{g},1}^S = 0 && \text{(20h)}
\end{aligned}$$

The non-anticipative constraint, (20h), stands only in the first time step, $k = 1$. It is because the given scenario ensembles of the water inflow are independent of each other. Therefore, the only initial state is a parent node. The weighting parameters in the objective function are set as shown in Table 2.

Table 2: Weight parameters in objective function

Parameter	1st optimizer	2nd optimizer
Q_{h}	1	1
$Q_{\Delta \mathrm{u}}$	100	0
Q_{V}	1000	0
Q_u	-	100

3.3 Simulation setup

For the simulation, the actual water inflow prediction and the historical power production plan data, stored by Skagerak Kraft, are used. Figure. 5 and Figure. 6 show the structure of the water inflow forecast and the historical power production plan. While all 50 scenario ensembles of inflow of Hjartsjå river are considered, the water inflow predictions of the three rivers between the reservoir and Omnessfossen(downstream) are simplified by considering the possible scenario of minimum flow rates.

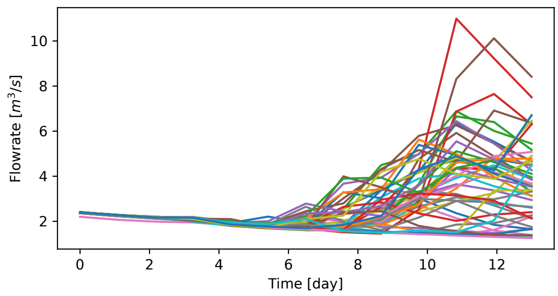

Figure 5: One example of the water inflow forecast

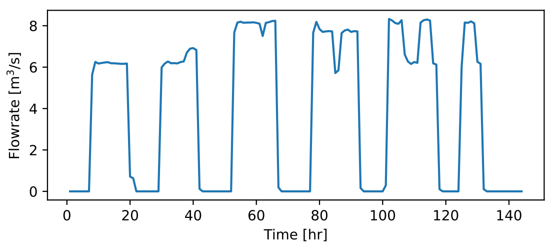

Figure 6: Historical water flow rate through the turbines for power production

For the simulation, the perfect model and the perfect prediction in power production are assumed. The simulation period is 5 days (144 hours) and the time step is set as 1 hour. The simulation is performed on CasAdi in Python Andersson et al. (2019). In the simulation, four different MPCs are tested as follows:

1. **Certainty-equivalent MPC**: the prediction horizon length is set as 13 days (312 hours) and utilizes the mean value of the water inflow forecast for the prediction of water inflow.
2. **Multistage MPC (MS13d)**: the prediction horizon length is set as 13 days (312 hours) and considers all the scenario ensembles for the optimization.
3. **Multistage MPC (MS6h)**; the prediction horizon length is set as 6 hours and considers all the scenario ensembles for the optimization.
4. **Stochastic Sequential MPC (Seq)**: the first optimizer has 13 days (312 hours) of the prediction horizon length and utilizes the mean value of the water inflow forecast to compute the reference control sequence. The second optimizer has 6 hours of the prediction horizon and considers all the possible scenarios of the water inflow for the optimization.

To assess the potential violations of the constraints by the realization of the different scenarios from the prediction, the open-loop robustness analysis is conducted. The process of the analysis is shown in Figure. 7. In the open-loop robustness analysis, the model is updated with the computed optimal control input and different water inflow from all the scenarios in an open-loop manner and checks whether the constraints are violated or not in the subsequent time step.

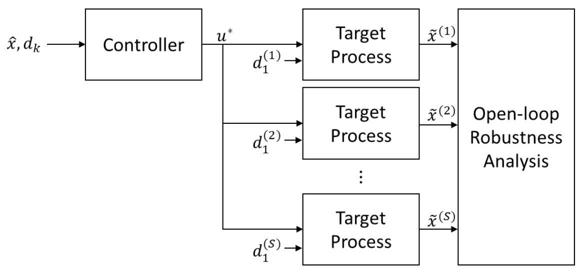

Figure 7: The procedure of open-loop robustness analysis

4 Simulation results and Discussion

Figure. 8 depicts the time-varying flow rate at the downstream location during the simulation period when the buffer reservoir is assumed to be absent. The figure highlights the occurrence of multiple hydropeaking events during the relatively short simulation period. To mitigate the potential damage caused by hydropeaking, it is imperative to optimize the operation of the buffer reservoir.

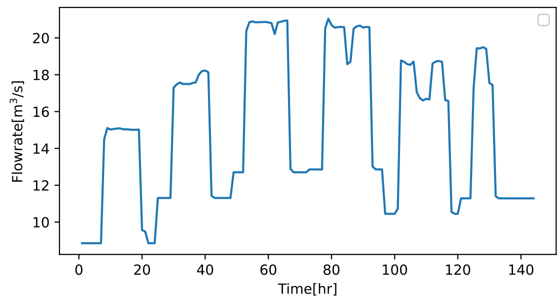

Figure 8: The flow rate at downstream under the assumption that a buffer reservoir does not exist

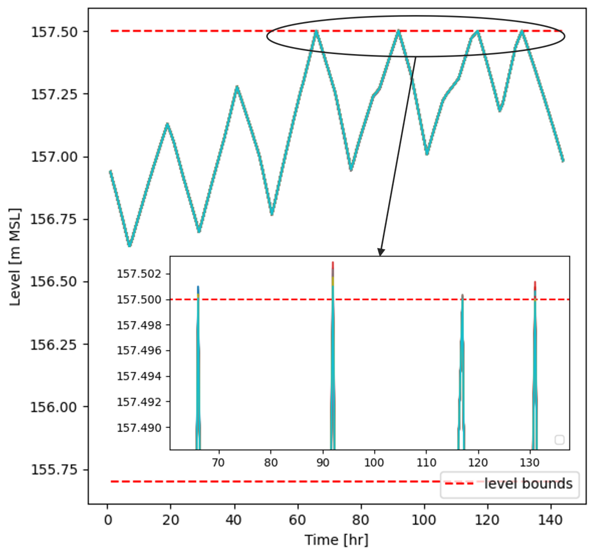

Figure 9: The result of the open-loop robustness analysis when the certainty equivalent MPC is implemented with the nominal values of the water inflow forecast

The simulation result of the certainty equivalent MPC and the open-loop robustness analysis is illustrated in Figure. 9, exhibiting the potential constraint violations at certain instances during the simulation period. It shows all the possible water level changes from all 50 possible scenario ensembles of water inflow. There are potential dangers of the constraint violations at 65 hours, 92 hours, 117 hours, and 131 hours during the simulation period. Although the water level surpasses the bound by small amounts, it is intolerable. However, these potential constraint violations are eliminated in the implementation of both the multistage MPC framework and the stochastic sequential MPC framework.

Figure. 10 shows the simulation results of three other MPC frameworks: the stochastic sequential MPC framework(**Seq**), the multistage MPC with 13 days of the prediction horizon length(**MS13d**), and the multistage MPC with 6 hours of the prediction horizon length (**MS6h**). Figure. 10(a) displays how the water level changes throughout the simulation period, Figure. 10(b) displays the gate openings (control input) throughout the simulation period, and Figure. 10(c) displays the flow rate at the downstream(Omnesfossen) during the simulation. The results of the sequential stochastic MPC are almost identical to that of the multistage MPC with 13 days of the prediction horizon length. For a fair comparison, the multistage MPC with 6 hours of the prediction horizon length (which is also equal to the prediction horizon length of the second optimizer for the sequential stochastic MPC) is displayed but it shows poor management of the water level, and the flow rate at downstream. The water level is unnecessarily lowered and the flow rate at downstream is not controlled constantly. It shows the importance of tracking the reference control sequence.

Table 3: The detail of computational time for each framework [s]

MPC	Mean	Max	Min
Certainty Equivalent	0.2804	0.6006	0.2128
Stochastic Sequential	0.3081	0.6246	0.2513
Multistage 13 days	27.09	68.65	13.87
Multistage 6 hours	0.1439	0.6497	0.0812

Table. 3 presents a comparison of the computational time required, in seconds, for solving each iteration of the optimization problem of the multistage MPC and stochastic sequential MPC for the buffer reservoir operation problem. It is observed that the stochastic sequential MPC reduces the computational time by 87 times compared to the multistage MPC with the prediction horizon length set to 13 days. Moreover, despite considering all 50 possible scenario ensembles, the computation time of the stochastic sequential MPC is found to be comparable to that of the certainty equivalent MPC.

Figure.11 demonstrates how the second optimization mitigates the impact of uncertainty. Specifically, Figure.11(a) displays the first control inputs of the control sequences from the first optimizer and the second optimizer of the stochastic sequential MPC framework during the simulation period. It reveals that there is no significant difference between the two control sequences, which is reasonable since the second optimizer is designed to track the reference control sequence from the first optimizer. However, when the first control inputs of the second optimizer are sub-

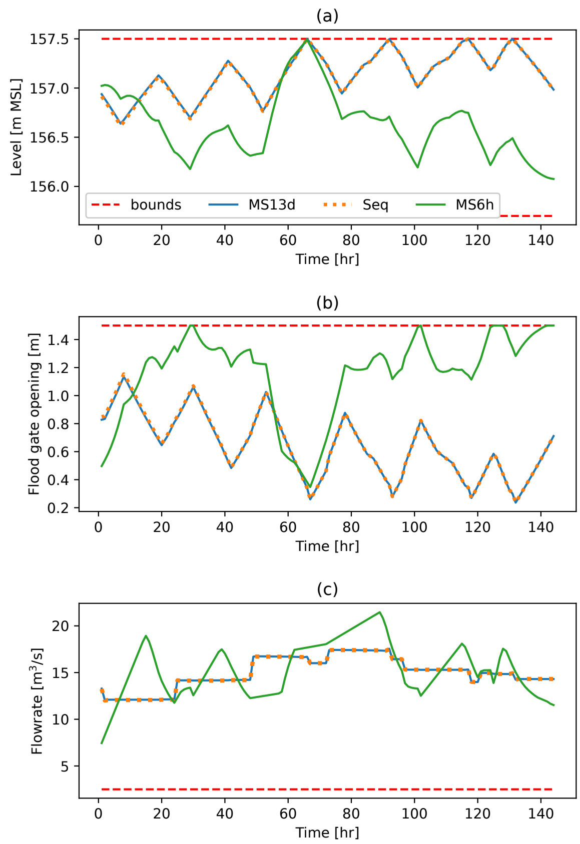

Figure 10: The comparison of the simulation results among the stochastic sequential MPC (**Seq**), the multistage MPC with different prediction horizon lengths of 6 hours (**MS6h**) and 13 days(**MS13d**): (a)The level changes throughout the simulation period, (b)The gate openings throughout the simulation period, and (c)The flow rate of the water at the downstream(Omnessfossen)

tracted from the first optimizer's first control inputs, as shown in Figure.11(b), it becomes apparent that the second optimizer increases the gate opening in certain instances. Notably, these instances align with the moments when the open-loop robustness analysis of the certainty equivalent MPC, shown in Figure.9, detects potential constraint violations. This finding confirms that the second optimizer adjusts the control sequence slightly to mitigate the impact of uncertainty effectively when required and when there is a possibility of violating constraints.

In flooding situations, the deviation of water inflow from one scenario to another increase significantly in the further future over the prediction horizon, leading to the potential infeasibility of OCP and, consequently,

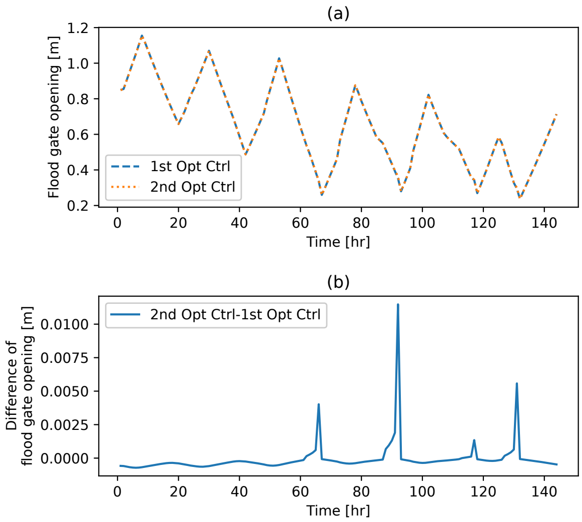

Figure 11: (a)The first control input from the first optimization and the second optimization of the stochastic sequential MPC framework, and (b)The difference of the first control input between the first and second optimization (The second optimization - the first optimization)

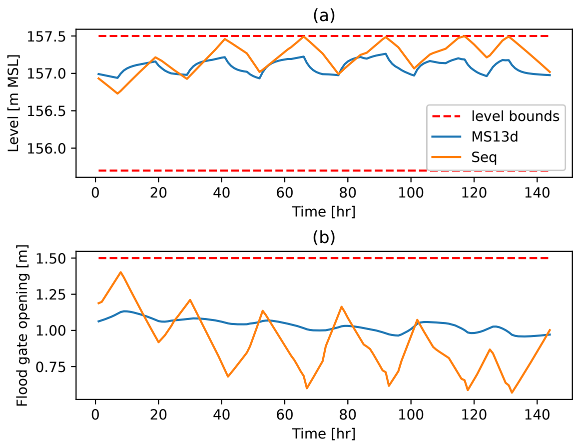

Figure 12: Simulation results of the stochastic sequential MPC(Prediction horizon: 1st optimizer:13days, 2nd optimizer:6hr) and multistage MPC(Prediction horizon: 13days) under assumption of the severe flooding situation. (a)The water level at the reservoir throughout the simulation period, and (b)The applied control inputs throughout the simulation period

unreasonable control actions. The simulation results of the stochastic sequential MPC and multistage MPC under severe flooding conditions are presented in Figure. 12. The results indicate that the multistage MPC fails to find an optimal solution, as the computation of OCP becomes infeasible, resulting in an inability to maximize the water level as desired. In contrast, the stochastic sequential MPC manages to find the optimal solution of OCP and effectively control the system in the desired manner. This highlights the better feasibility of the stochastic sequential MPC in solving OCP as it does not consider the deviations of the water inflow in the long-term future, which can be compensated by the feedback control concept.

5 Conclusion

This study utilizes the stochastic sequential MPC framework for controlling the buffer reservoir in the Hjartdøla hydropower system under uncertainty. Compared to the certainty equivalent MPC, which fails to account for uncertainty, and the multistage MPC, which has slower computation time, the stochastic sequential MPC effectively handles uncertainty and ensures that no constraint violations occur. The second optimizer in the stochastic sequential MPC framework is shown to counteract the influence of uncertainty by slightly adjusting the control sequence when necessary, as evidenced by simulation results. Moreover, the stochastic sequential MPC demonstrates significantly faster computation time in Table. 3 and better feasibility in solving OCP in the severe flooding situation. These advantages are attributed to the first optimizer providing a reference control sequence to the second optimizer, which reduces computational demand while reflecting the trend of future uncertainty information. Overall, the results suggest that the stochastic sequential MPC framework is a promising approach for real-time control of hydropower systems under uncertainty.

References

Andersson, J. A. E., Gillis, J., Horn, G., Rawlings, J. B., and Diehl, M. CasADi – A software framework for nonlinear optimization and optimal control. *Mathematical Programming Computation*, 2019. 11(1):1–36. doi:10.1007/s12532-018-0139-4.

Batalla, R. J., Gibbins, C. N., Alcázar, J., Brasington, J., Buendia, C., Garcia, C., Llena, M., López, R., Palau, A., Rennie, C., Wheaton, J. M., and Vericat, D. Hydropeaked rivers need attention. *Environmental research letters*, 2021. 16(2):21001. doi:10.1088/1748-9326/abce26.

IEA. Hydropower special market report—analysis and forecast to 2030. `https://www.iea.org/reports/hydropower-special-market-report,License:CCBY4.0`, 2021.

Jeong, C., Furenes, B., and Sharma, R. MPC operation with improved optimal control problem at dalsfoss power plant. *Proceedings of SIMS EUROSIM conference 2021*, 2021. 11(1):226–233. doi:10.3384/ecp21185226.

Jeong, C., Furenes, B., and Sharma, R. Implementation of simplified sequential stochastic model predictive control for operation of hydropower system under uncertainty. *Computers & Chemical Engineering*, 2023a. 179:108409. doi:10.1016/j.compchemeng.2023.108409.

Jeong, C., Furenes, B., and Sharma, R. Multistage Model Predictive Control with Simplified Scenario Ensembles for Robust Control of Hydropower Station. *Modeling, Identification and Control*, 2023b. 44(2):43–54. doi:10.4173/mic.2023.2.1.

Jeong, C. and Sharma, R. Stochastic mpc for optimal operation of hydropower station under uncertainty. *IFAC PapersOnLine*, 2022a. 55(7):155–160. doi:10.1016/j.ifacol.2022.07.437.

Jeong, C. and Sharma, R. Tuning model predictive control for rigorous operation of the dalsfoss hydropower plant. *Energies (Basel)*, 2022b. 15(22):8678. doi:10.3390/en15228678.

Jeong, C. and Sharma, R. Multistage model predictive control with simplified method on scenario ensembles of uncertainty for hjartdøla hydropower system. In *2023 IEEE Conference on Control Technology and Applications (CCTA)*. pages 733–740, 2023. doi:10.1109/CCTA54093.2023.10252685.

Klintberg, E., Dahl, J., Fredriksson, J., and Gros, S. An improved dual newton strategy for scenario-tree mpc. *2016 IEEE 55th Conference on Decision and Control (CDC)*, 2016. pages 3675–3681. doi:10.1109/CDC.2016.7798822.

Langhans, S. D., Jähnig, S. C., Lago, M., Schmidt-Kloiber, A., and Hein, T. The potential of ecosystem-based management to integrate biodiversity conservation and ecosystem service provision in aquatic ecosystems. *The Science of the total environment*, 2019. 672:1017–1020. doi:10.1016/j.scitotenv.2019.04.025.

Lucia, S., Finkler, T., and Engell, S. Multi-stage nonlinear model predictive control applied to a semi-batch polymerization reactor under uncertainty. *Journal of Process Control*, 2013. 23(9):1306–1319. doi:10.1016/j.jprocont.2013.08.008.

Maiworm, M., Bäthge, T., and Findeisen, R. Scenario-based model predictive control: Recursive feasibility and stability. In *IFAC-PapersOnLine*, volume 48. pages 50–56, 2015. doi:10.1016/j.ifacol.2015.08.156.

Martí, R., Lucia, S., Sarabia, D., Paulen, R., Engell, S., and de Prada, C. Improving scenario decomposition algorithms for robust nonlinear model predictive control. *Computers chemical engineering*, 2015. 79:30–45. doi:10.1016/j.compchemeng.2015.04.024.

Mayne, D., Rawlings, J., Rao, C., and Scokaert, P. Constrained model predictive control: Stability and optimality. *Automatica (Oxford)*, 2000. 36(6):789–814. doi:10.1016/S0005-1098(99)00214-9.

Mesbah, A. Stochastic model predictive control: An overview and perspectives for future research. *IEEE control systems*, 2016. 36(6):30–44. doi:10.1109/MCS.2016.2602087.

Morari, M. and Lee, J. H. Model predictive control : past, present and future. *Computers chemical engineering*, 1999. 23(4-5):667–682. doi:10.1016/S0098-1354(98)00301-9.

NVE. Supervision of dams, (accessed: 24.10.2022). `https://www.nve.no/supervision-of-dams/?ref=mainmenu`, 2022.

Schmutz, S. and Sendzimir, J. *Riverine Ecosystem Management : Science For Governing Towards a Sustainable Future (Volume 8.0)*, volume 8 of *Aquatic Ecology Series*. Springer Open, Cham, 2018. doi:10.1007/978-3-319-73250-3.

Scokaert, P. and Mayne, D. Min-max feedback model predictive control for constrained linear systems. *IEEE transactions on automatic control*, 1998. 43(8):1136–1142. doi:10.1109/9.704989.

SkagerakKraft. Kraftverk - kraftverksoversikt - hjartdøla, (accessed: 24.10.2022). `https://www.skagerakkraft.no/hjartdola/category1382.html`, 2022.